

AIAA 79-1741R

Sensing the Position and Vibration of Spacecraft Structures

R.H. Anderson,* C-C. Huang,† and N.E. Buholz‡
Lockheed Missiles & Space Company, Inc., Sunnyvale, Calif.

The authors are involved in the development of a family of laser heterodyne sensors for use in the active control of spacecraft structures. These sensors include a HeNe distance measuring system for structures requiring accuracies to 0.1 mm, and a CO₂ distance measuring system which will measure unambiguously down to 0.01 μm . Vibration sensors based on both HeNe and CO₂ lasers are also being developed. These systems will measure fractions of a μm displacement from dc to kHz. This paper discusses the design theory and tradeoffs required for instrument selection.

Nomenclature

A	= $\pi \times$ modulation depth
B	= electronic bandwidth
$h\nu$	= photon energy
k	= Boltzman's constant
P_l	= optical local oscillator power
P_n	= dc signal power ($n = 1, 2, \dots$)
P_s	= optical signal power
q	= electron charge
R	= range
R_L	= resistance of load resistor
S/N	= signal-to-noise ratio
t	= time
T_A	= equivalent temperature of amp
λ_m	= modulation wavelength
λ_o	= optical wavelength
η	= detector quantum efficiency
ϕ_a, ϕ_M	= phase constants
ϕ_m	= range-related modulation phase = $4\pi R/\lambda_m$
ϕ_o	= range-related optical phase = $4\pi R/\lambda_o$
ω_a	= angular frequency of acoustic wave driving dual Bragg cell
ω_m	= angular frequency of phase modulation
ν	= frequency

Introduction

FOR several years the authors have been developing sensors to be used for the measurement and active control of spacecraft structures. These sensors are all laser heterodyne systems. Both HeNe and CO₂ lasers have been used. All of these sensors have been breadboarded to verify performance and are in various stages of development directed toward prototype engineering models.

A coarse system, which is designed for applications where high accuracy is not required, uses a modulated beam and a high-accuracy phase measurement scheme to obtain resolution on the order of 0.1 mm. With several modulation frequencies, distances on the order of kilometers can be measured. A fine measurement system has been developed that will work either in conjunction with the coarse system or independently. It uses a multistate two-color CO₂ laser which can be used to produce unambiguous measurements from 20 cm down to 0.01 μm resolution over distances to 100 m.

A summary of the distance-measuring capabilities is illustrated in Table 1. This table gives the approximate range

covered by the different modes of each sensor. The first three are achieved by impressing different modulation frequencies on the coarse sensor. The last five are achieved by working through a hierarchy of frequencies obtained from the four states of operation for the two-color CO₂ laser used in the fine system.

Deployment of these measuring systems is very dependent upon the application. A typical example is the coarse system used to monitor the figure of an antenna, as illustrated in Fig. 1. The fine system requires special beam-directing techniques discussed later with Fig. 7. For the vibration sensor, up to 50 separate beams can be brought out in parallel and directed toward the points to be monitored. Care must be taken to separate beam director vibrations from structural vibrations.

Vibration measurements have been made using both doppler frequency detection and a beat frequency phase measurement system with capabilities of measuring displacements less than a 0.1 μm at vibration frequencies from essentially dc to several kHz.

All of the sensors described herein use Bragg cells. These are acousto-optical devices which, when a frequency is applied, produce a moving diffraction grating across the optical beam in the cell. The beam sent in is partially diffracted and frequency shifted, providing an output which is spatially separated (in angle) and frequency shifted from a throughput beam which is straight through and unshifted in frequency. When several frequencies are applied, several outputs are produced, each spatially and frequency separated.

Coarse Measurements

The coarse system measures distance by accurately measuring the phase of a modulated laser beam. Distance to a reference point is compared with the distance to the target. This method eliminates, through common moding, any drifts prior to the output beamsplitter. Actual implementation of both CO₂ and HeNe systems has been accomplished. The following discussion applies to both systems.

An optical layout and signal processing flow are illustrated in Fig. 2. The beam from the laser is both spatially and frequency shifted by the Bragg cell. The unshifted portion of the beam is used as the local oscillator for the heterodyne receiver. The shifted beam is directed through the phase modulator with mode matching lenses. This modulated beam is split, with one beam sent to the reference mirror and the other to the target. The beams are sampled alternately, 180 deg out of phase, for signal processing. Both the reference beam and target beam are returned to combine with the local oscillator beam than be received by the detector.

The processing electronics consist of the system to be described, as well as a microprocessor for converting the signals to a digital range output. The signal processing scheme described in this section has been breadboarded and its performance demonstrated.

Presented as Paper 79-1741 at the AIAA Guidance and Control Conference, Boulder, Colo., Aug. 6-8, 1979; submitted Oct. 30, 1979; revision received July 28, 1980. Copyright © American Institute of Aeronautics and Astronautics, Inc., 1980. All rights reserved.

*Project Leader, Sensor Technology Space Systems Div

†Research Scientist, Sensor Technology Space Systems Div.

Table 1 Measurement ranges

Measurement technique ^a	Distance meters										
	10 ³	10 ²	10 ¹	10 ⁰	10 ⁻¹	10 ⁻²	10 ⁻³	10 ⁻⁴	10 ⁻⁵	10 ⁻⁶	10 ⁻⁷
Coarse 1 MHz mod											
Coarse 100 MHz mod											
Coarse 500 MHz mod											
Fine syn. wavelength III											
Fine syn. wavelength II											
Fine syn. wavelength I											
Fine diff. fringe											
Fine fractional fringe											

^aVibration measurement system demonstrated with 0.05 m-Hz (displacement-frequency product) capability, 0.08 μ m resolution from dc to kHz.

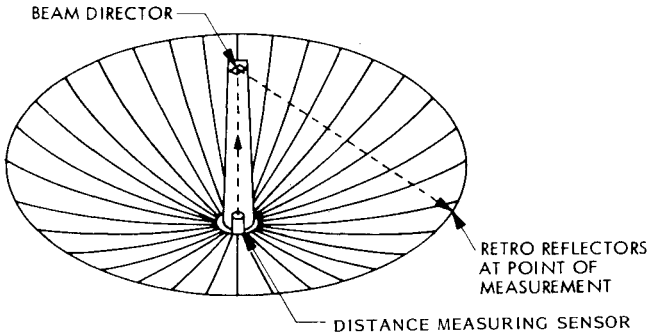


Fig. 1 Coarse sensor deployment.

The processing flow is shown in Fig. 2. Beginning in the upper left-hand corner, FM modulation frequencies of 1.0 or 100 MHz are selectable by the rf switch. The selected rf power is divided and the first fraction passes successively through an adjustable (phase shifting) transmission line, a power amplifier, and a phase modulator for the working beam. The other fraction of the rf power passes to the 90-deg hybrid, where about one-half the power is phase shifted and two outputs corresponding to sine and cosine functions are provided. These outputs, each with a phase and amplitude trimmer, go to the inputs of a pair of SPST rf switches. The switch output provides the following rf mixer with sine and cosine inputs on alternate half-cycles. The crystal detector, amplifier, and logarithmic voltmeter provide the output shown.

Observe in Fig. 2 that phase shifting is used to move the observation close to a phase angle of 45 deg or 45 deg $\pm N \times 90$ deg. The phase shifting can be accomplished by several methods and the switching of calibrated delay lines is a case in point. Whatever technique is used requires that the phase shift calibration and stability be compatible with the range resolution required. For the case of switched delay lines used as an example, this applies to both delay lines and the switches.

Observation of delay line and switch stability has been made for the 100 MHz amplitude modulation case. The stability has been found compatible with the range resolution requirements discussed previously.

Photomixing the optical local oscillator and target-sensing beams produces signal components (two sidebands) consisting of a mix between the dual Bragg cell-generated acoustic frequency and the electro-optic modulator phase modulation frequency (carrying range information) of the following form:

$$\cos[(\omega_m + \omega_a)t - (\phi_o - \phi_a) + (\phi_m - \phi_M)]$$

$$\cos[(\omega_m - \omega_a)t + (\phi_o - \phi_a) + (\phi_m - \phi_M)]$$

Suppose we mix these two sidebands (at frequencies $\omega_m + \omega_a$ and $\omega_m - \omega_a$) with $\cos\omega_m t$ and $\sin\omega_m t$, alternately

(which are derived from a 90-deg hybrid power divider), by using an rf mixer. Then the output of the rf mixer will contain $\sin(\phi_m - \phi_M) \sin(\omega_a t + \phi_o - \phi_a)$ and $\cos(\phi_m - \phi_M) \sin(\omega_a t + \phi_o - \phi_a)$, alternately. If we take the amplitude ratio of these two alternate signals, a range-related function $\tan(\phi_m - \phi_M) = \tan(4\pi R/\lambda_m - \phi_M)$ will be obtained. Since we take the ratio of two rf mixer outputs to obtain range function, any variation of signal power, electronic gain, etc., is common to both outputs and is cancelled. The theoretical details on range function and range resolution derivations are described in the following paragraphs.

With a dual Bragg cell used, the laser output at frequency ω_o is frequency shifted to $\omega_o - \omega_a$. The frequency unshifted beam is employed as the optical local oscillator (LO). After passing through the phase modulator, the frequency shifted beam is directed alternately to the target and reference mirrors at ranges R_t and R_r , respectively. An optical chopper may be employed to select alternately between the target and reference beams. Upon return, the distance-measuring beam is made congruent with the LO beam and photodetected. The output of the photodetector is amplified and sent through a notch filter centered at frequency ω_a before reaching the RF mixer.

A 90-deg hybrid power divider employs a portion of the output of the oscillator at ω_m and presents two signals with a 90-deg phase difference to a SPDT rf switch and, in turn, to an rf mixer. The inputs combined by the mixer from the signals $\sin(\phi_m - \phi_M) \sin(\omega_a t + \phi_o - \phi_a)$ and $\cos(\phi_m - \phi_M) \sin(\omega_a t + \phi_o - \phi_a)$ according to whether the rf switch is passing $\cos\omega_m t$ or $\sin\omega_m t$. The bandpass filter selects only those spectral components at frequency ω_a . The output of a square law crystal detector thus consists of signals with amplitudes $\sin^2(\phi_m - \phi_M)$ or $\cos^2(\phi_m - \phi_M)$. By taking the logarithmic difference of these two signals, we obtain:

$$\begin{aligned} 10 \log[\sin^2(\phi_m - \phi_M)] - 10 \log[\cos^2(\phi_m - \phi_M)] \\ = 10 \log[\tan^2(\phi_m(R) - \phi_M)] \end{aligned}$$

The range R can be solved for explicitly in a simple straightforward manner. The target range relative to the reference mirror can be calculated by subtracting two consecutive range measurements, one to the target and another to the reference mirror. From Refs. 1 and 2, the range resolution is found to be

$$(\Delta R_m)_{\min} = \frac{\lambda_m}{4} (\Delta \phi_m)_{\min} = \frac{\lambda_m}{\pi A \sqrt{2(S/N)}}$$

$$\frac{S}{N} \approx \frac{2 \left(\frac{\eta q}{h \nu} \right)^2 P_i P_s}{B \left(\frac{2 q^2 \eta}{h \nu} P_i + \frac{4 k T_A}{R_L} \right)}$$

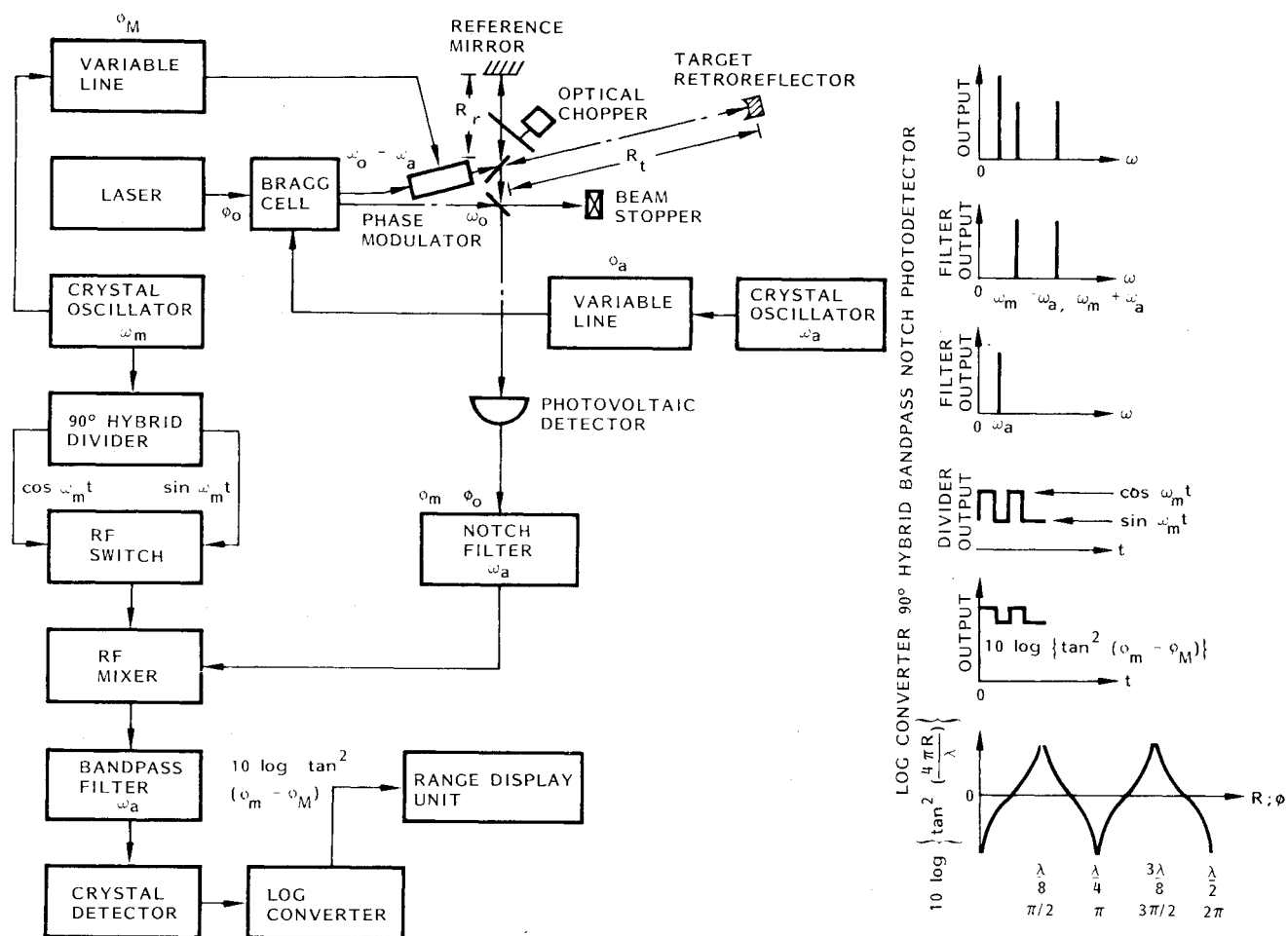


Fig. 2 Coarse sensor signal processing.

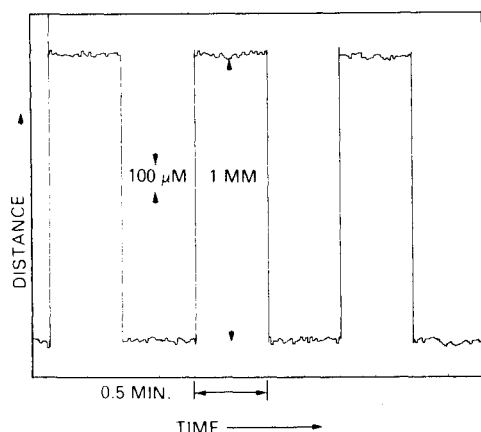
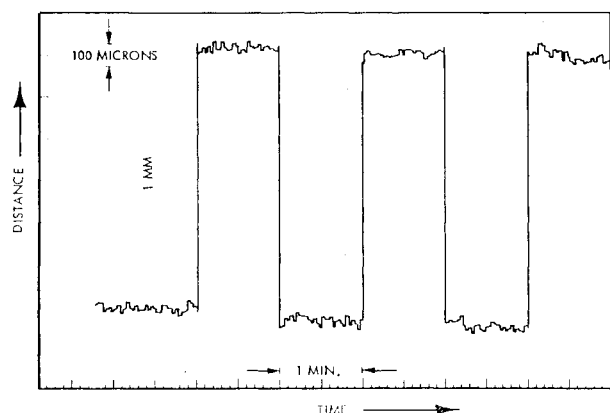


Fig. 3 Coarse sensor data.

Table 2 Parameters for range resolution calculation

Parameters	HeNe system	CO ₂ system
λ_m, m		3
Modulation depth	0.2	0.02
η	0.8	0.5
q, C	0.8	1.6×10^{-19}
$h\nu, J$	3.13×10^{-19}	1.87×10^{-20}
P_i, W		10^{-3}
P_s, W		10^{-6}
B, Hz		10^3
$k, J/K$		1.38×10^{-23}
T_A, K		596 ^a
R_L, Ω		50

^a For an amplifier with 3 dB noise figure which implies

$$\frac{(\Delta R_m)_{CO_2}}{(\Delta R_m)_{HeNe}} = \frac{65.5 \mu m}{52.5 \mu m} = 1.25.$$

The range of resolution of an HeNe system is found to be comparable with that for a CO₂ system for the typical parameters listed in Table 2.

Range resolution can be improved by a factor \sqrt{BT} for a given integration time T and electronic bandwidth B . Subsequent to integration, the theoretically derived range resolution for a data rate of one reading per second is 1.66 and 2.07 μm for HeNe and CO₂, respectively.

Figure 3 illustrates three examples of coarse system data. The outputs are 1-s time averages of data showing the system resolution capability. Figure 3a is a CO₂ system modulated at 100 MHz and Fig. 3b is an HeNe system modulated at 400 MHz.

As can be seen from this data, the rms noise is approaching the theoretical limit. The data was taken in an open lab with minimal vibration isolation.

Fine Measurements

The heart of the fine measurement system is the switchable two-color CO₂ laser. Gain occurs in the CO₂ gas mixture in many distinct lines corresponding to a given vibrational transition frequency. These lines, corresponding to *R* and *P* branches, and numbered in each, are illustrated in Fig. 4.

By controlling the cavity length, as described in Ref. 3, the line of operation can be established. If the length is such that an *R* frequency and a *P* frequency have the same gain, they will operate simultaneously. This can be accomplished by separation of the signals (spectrally) and servoing a piezoelectric driven mirror to the proper cavity length. Thus, two-color operation is achieved. This can be refined further by selecting a specific *R* line and *P* line within the branches for

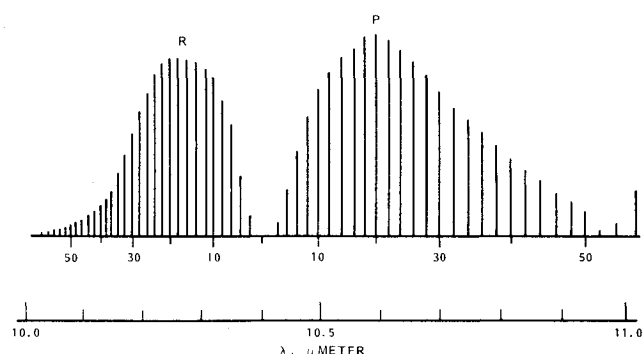


Fig. 4 CO₂ gain curve, 10.4 μm band.

laser operation. A laser has been developed which can be switched through four pairs of lines.

By obtaining the difference frequency between pairs of lines, longer wavelengths can be produced. By looking at the difference between a pair of differential fringes, still longer wavelengths occur. In Fig. 5, a hierarchy of wavelengths is established which can be obtained from the laser. The differential fringes are those obtained from a single two-color state. The synthetic wavelengths only exist in the comparison of one state to another. From this, it can be seen that an ambiguity of 40 cm can be obtained in total path length (20 cm in measuring distance). This operation is described in more detail in Ref. 4.

Two types of phase measurement techniques have been used. If the position sensor is to include the coarse system, then a similar processing scheme can be used. For this system, the rf switch is operated at ω_a and the mixer input is filtered to allow ω_o in. The resulting output is $10 \log \{ \tan^2 (\phi_o - \phi_a) \}$, where a variable line has now been used for the ω_a in Fig. 6.

These systems operate simultaneously producing the coarse and fine data. The theoretical range resolution for this scheme is 0.0008 μm for a 3 kHz bandwidth. This has not been accomplished due to internal optical contamination, but better than 0.01 μm has been achieved.

An alternate phase measurement scheme, described in Ref. 4, for the fine system only, which employs a digital zero crossing phase comparison has been used and it, too, is able to achieve a distance resolution of 0.01 μm.

The optical layout of the fine system is illustrated in Fig. 7. A beam-directing scheme needed to be devised that would not affect the path length. That scheme is also shown in Fig. 7, where all errors occurring behind the output beamsplitter are common-moded in the reference and target measurements. It will require calibration of all measurement positions to account for optical differences, but no scanner-induced errors should occur.

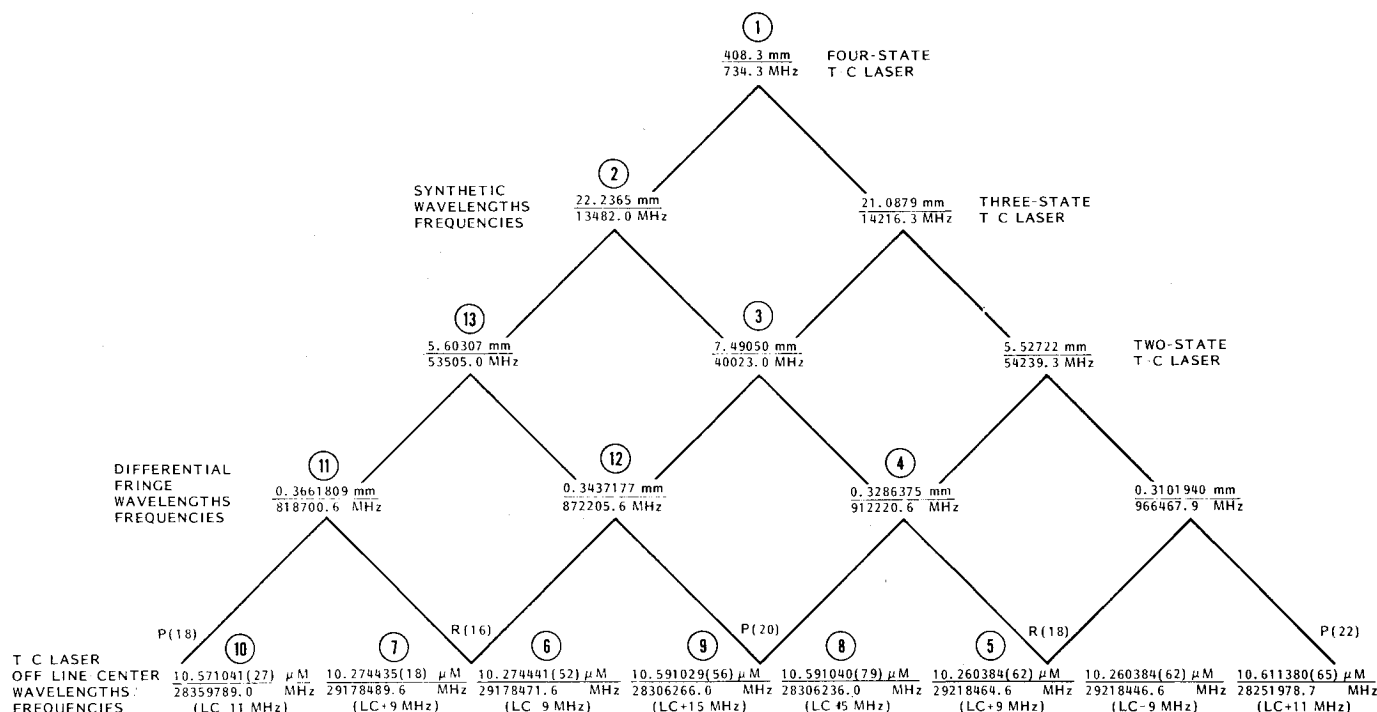


Fig. 5 Wavelength hierarchy pyramid.

Fig. 6 Coarse and fine system combined signal processing.

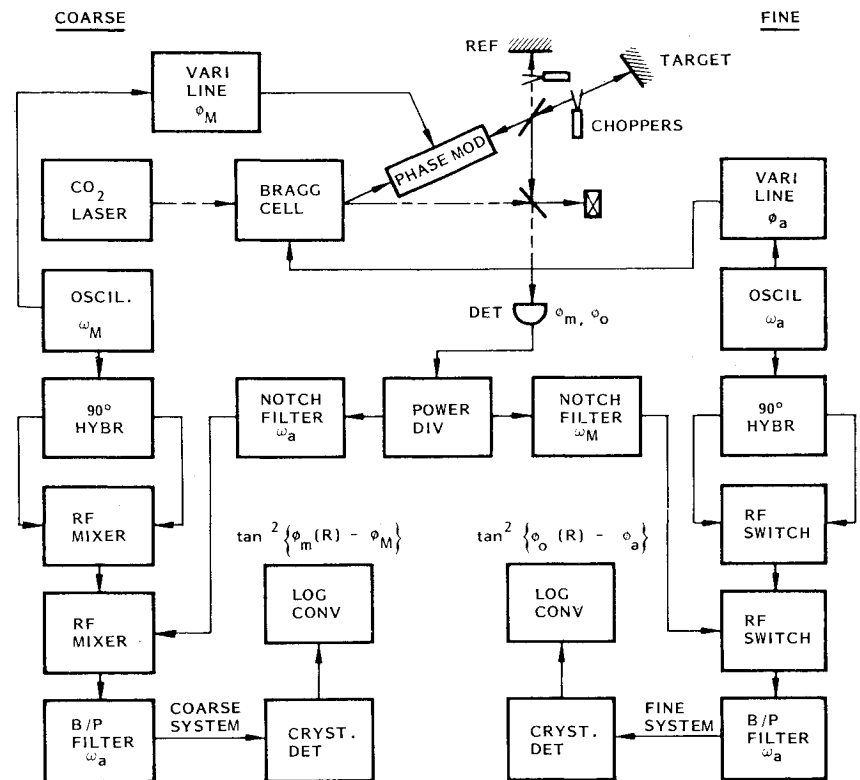
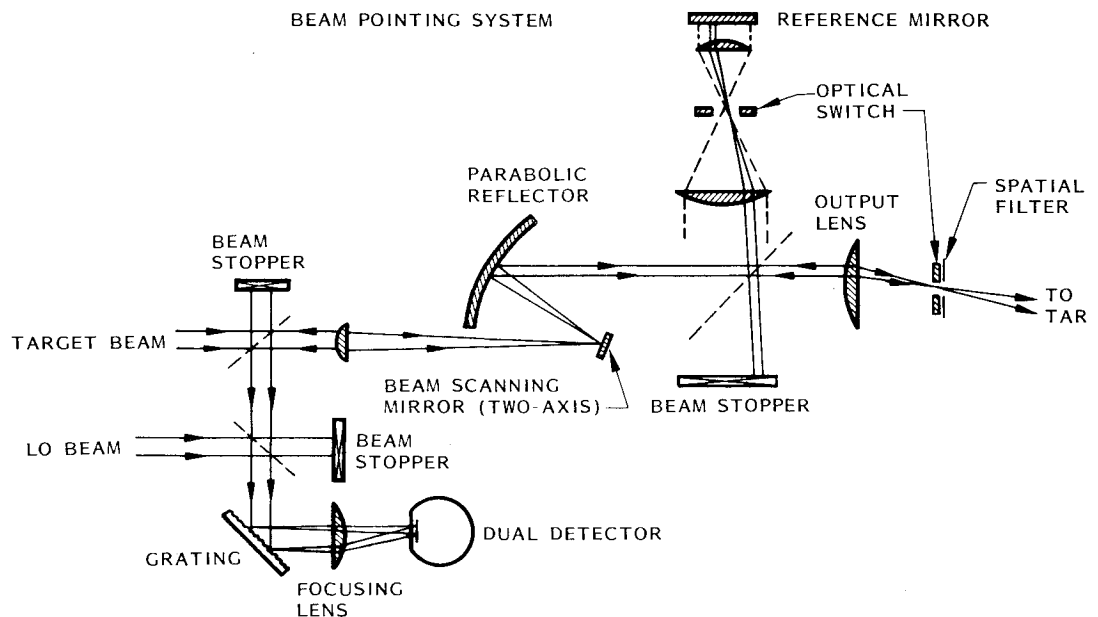


Fig. 7 Fine system output scanner.



Typical performance data for the fine system is illustrated in Fig. 8. The sensor tracked a target moved out and back a distance of 1.5 m. At the same time, a Hewlett-Packard interferometer was used to track the same target with a congruent beam. The data represents the difference in output of the two systems. The slope can be accounted for by slight inaccuracies in the atmospheric corrections used.

Vibration Measurements

A HeNe laser vibration sensor⁵ has been demonstrated which features analog and digital outputs for computational convenience, and which complements conventional vibration sensors (i.e., accelerometers) by sensing vibratory events at low frequencies from dc to beyond a kHz. Vibration amplitude resolution of the sensor is 0.08 μm , maximum am-

plitude and frequency product is 0.05 m-Hz for a 2 MHz electronic bandwidth. For example, the maximum measurable vibration amplitude for a 25 Hz vibration is 2 mm. The time delay of the sensor output from the actual vibration is less than 2 μs , which is essentially real time for measuring the dynamics of structures and vibration sensing for the dynamic damping of structures (active control). By electronically splitting the laser beam using a Bragg cell, it is possible to simultaneously sample and, hence, monitor a large number of points to which retroreflectors have been affixed. Although the laboratory vibration sensor employed but two channels, it exhibited the basis for continuously sensing more than 50 independent vibrating targets.

The vibration sensor employs a low-power HeNe laser and two Bragg cells—one to provide a heterodyne offset

frequency for use as a local oscillator, the other for generating multiple beams for various targets. Optical path variations due to the vibratory motion of each target is measured by comparing zero-crossings of the local oscillator signal with those of each target, identifiable by a specific Bragg frequency. The various differential zero-crossings provide the basis for the digital output of the vibration sensor. Experimental results compare well with theoretical predictions.

The vibration sensor conceptual layout diagram is illustrated in Fig. 9. The first Bragg cell translates the laser output frequency from ν_0 to $\nu_0 + \nu_a$. The frequency-translated beam is directed by the second Bragg cell to two target retroreflectors which correspond to two driving frequencies, ν_1 and ν_2 , respectively. The laser beam incident upon the channel 1 target at range Y_1 has a frequency $\nu_0 + \nu_a + \nu_1$, which is different from the frequency $\nu_0 + \nu_a + \nu_a$ for the laser beam on the channel 2 target at range $Y_2(t)$. The returning signals $\nu_0 + \nu_a + \nu_1 + 2Y_1/\lambda$, where λ is the laser wavelength, are being shifted in frequency, when returned through the second Bragg cell, by ν_1 and ν_2 , respectively. A photodiode detector is used to sense the heterodyne beat between the optical local oscillator (LO) beam, which is derived from the laser output directly, and the vibration sensing beams.

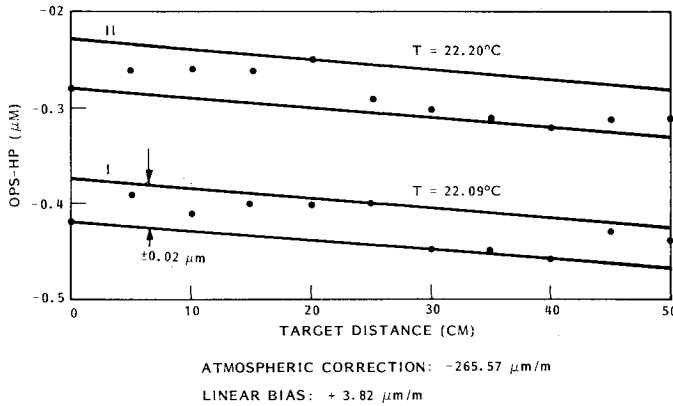


Fig. 8 Fine system data.

In order to separate two target signals from the photodetector output, we can first mix it with $\cos[2\pi(\nu_a - \nu_r)t]$ to obtain $\cos[2\pi(2\nu_1 + \nu_r)t + 4\pi Y_1/\lambda]$ and $\cos[2\pi(2\nu_2 + \nu_r)t + 4\pi Y_2/\lambda]$. We can then mix these with $\cos[2\pi(2\nu_1)t]$ to obtain $\cos[2\pi\nu_r t + 4\pi Y_1/\lambda]$, and with $\cos[2\pi(2\nu_2)t]$ to obtain $\cos[2\pi\nu_r t + 4\pi Y_2/\lambda]$. Here, ν_r is the frequency of the reference signal which, in this case, is 4 MHz. The signal $\cos[2\pi(\nu_a - \nu_r)t]$ is a result of mixing the reference signal with the first Bragg cell driving signal and bandpassing at $\nu_a - \nu_r$. Signals $\cos[2\pi(2\nu_1)t]$ and $\cos[2\pi(2\nu_2)t]$ are derived from frequency doublers and, in turn, from oscillators at frequencies ν_1 and ν_2 , respectively.

Signals of both channels are centered at frequency ν_r , but separately passed by each bandpass filter. The digital signal processor takes the reference signal and the output of two channels from the bandpass filters to process the vibration information of the targets. By comparing the zero-crossings of $\cos(2\pi\nu_r t)$ with $\cos(2\pi\nu_r t + 4\pi Y_1/\lambda)$ and $\cos(2\pi\nu_r t + 4\pi Y_2/\lambda)$, the displacement ΔY_1 and ΔY_2 can easily be determined. For every zero crossing count difference, there is a phase change of 2π rad or a displacement of $\lambda/2 = 0.32 \mu\text{m}$. When four reference signals— $\cos(2\pi\nu_r t)$, $\cos(2\pi\nu_r t + \pi/2)$, $\cos(2\pi\nu_r t + \pi)$, and $\cos(2\pi\nu_r t + 3\pi/2)$ —are used for zero-crossing comparison, the displacement resolution is $\lambda/8$ or $0.08 \mu\text{m}$.

The power signal-to-noise ratio S/N , of the sensor is

$$\left(\frac{S}{N}\right)_1 = \frac{I_{s1}^2}{I_N^2} \approx \frac{2\left(\frac{\eta q}{h\nu}\right)^2 P_1 P_i}{B\left(\frac{2\eta q^2}{h} P_i + \frac{4kT_A}{R_L}\right)}$$

for channel 1 target and

$$\left(\frac{S}{N}\right)_2 = \frac{I_{s2}^2}{I_N^2} \approx \frac{2\left(\frac{\eta q}{h\nu}\right)^2 P_2 P_i}{B\left(\frac{2\eta q^2}{h\nu} P_i + \frac{4kT_A}{R_L}\right)}$$

for channel 2 target.

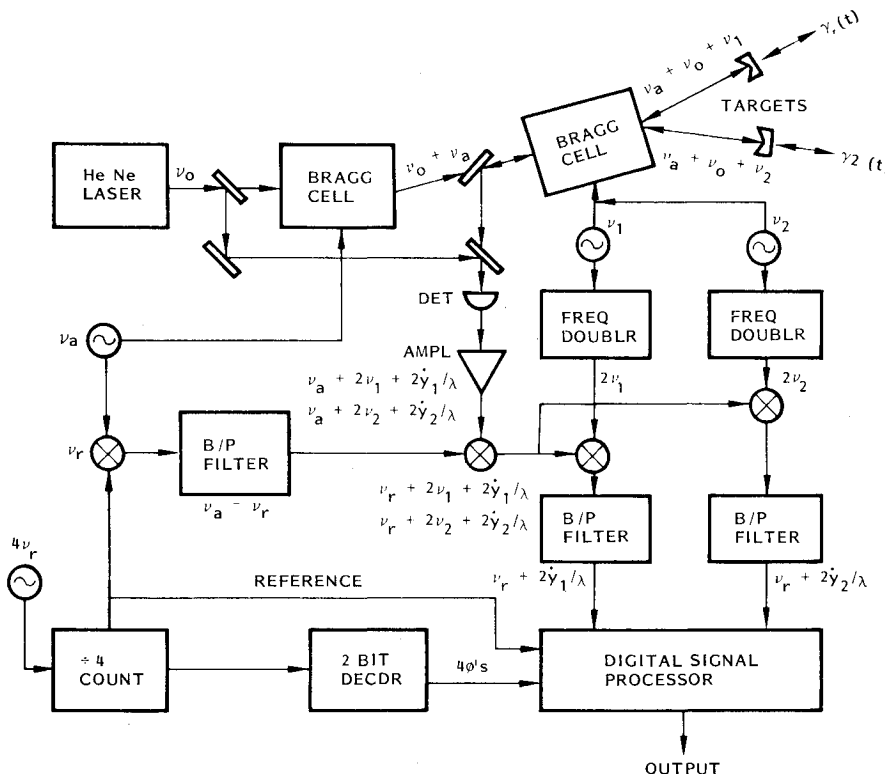


Fig. 9 Vibration sensor signal processing.

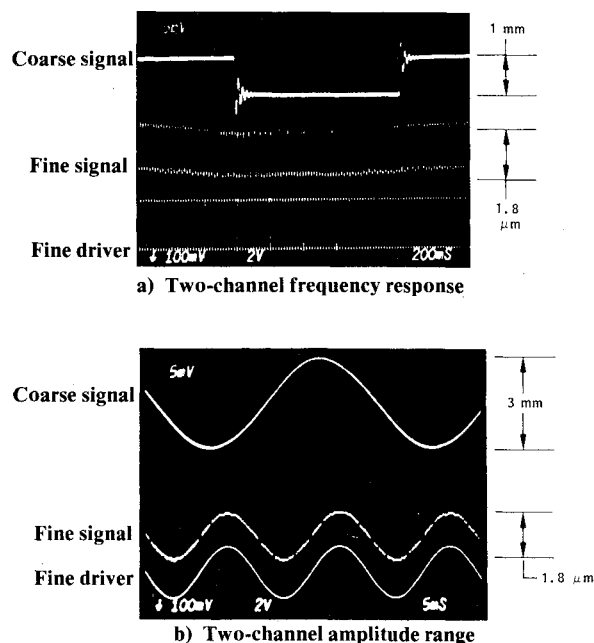


Fig. 10 Vibration sensor data.

Assuming a 0.4 mW single-frequency HeNe laser is used to measure vibrations of 50 targets, the signal-to-noise ratio of each channel can be calculated according to the following typical values:

$$\begin{aligned} \eta &= 0.8 & B &= 2 \times 10^6 \text{ Hz} \\ q &= 1.6 \times 10^{-19} \text{ C} & k &= 1.38 \times 10^{-23} \text{ J/K} \\ h\nu &= 3.13 \times 10^{-17} \text{ J} & T_A &= 596 \text{ K} \\ P_I &= 10^{-4} \text{ W} & R_L &= 50 \Omega \\ P_I &= 5 \times 10^{-9} \text{ W} \end{aligned}$$

yielding the result $S/N = 123$.

This signal-to-noise ratio is more than what is required by the signal digital processor to process the signal. For a constant signal-to-noise ratio, the maximum number of channels which can be measured by the sensor is proportional to the laser output power.

The doppler frequency, $\nu_{dl} = 2Y_l(t)/\lambda$, for a sinusoidal vibration can be written as $\nu_{dl} = 4\pi\nu_{ml}Y_{dl}\sin(2\pi\nu_{ml}t)/\lambda$, where ν_{ml} is the modulation frequency and Y_{dl} is the amplitude of vibration. For a 2 MHz bandwidth, the peak doppler frequency is limited to 1 MHz or $4\pi\nu_{ml}Y_{dl}/\lambda = 10^6 \text{ Hz}$ or $\nu_{ml}Y_{dl} = 0.05 \text{ m-Hz}$. Therefore, the maximum amplitude and frequency product of the vibratory targets is limited to 0.05 m-Hz for 2 MHz electronic bandwidth.

Vibration sensor data is shown in Fig. 10 for a two-channel system. Figure 10a shows one channel operating at 30 Hz, 3 mm peak-to-peak. The digital resolution of $0.08 \mu\text{m}$ is detectable in the latter channel. The bottom trace is the piezoelectric drive signal for the 60 Hz, showing negligible phase shift. Figure 10b has the same outputs with a square wave applied to the first channel to illustrate dc performance. The ringing in the signal is caused by the transducer motion.

Conclusions

Based on the above analyses and the breadboard demonstrations performed, we have made the following conclusions:

- 1) It is possible to measure distance with HeNe absolutely from kilometers down to 0.1 mm.
- 2) It is possible to measure distance with CO_2 from kilometers down to $0.01 \mu\text{m}$.
- 3) Rates on the above measurements can be made from rates of 1 per sec to 100 per sec.
- 4) It is possible to measure vibrations from dc to kHz with up to 50 channels per detector/laser.

The primary concern in the application of the above sensors is one of beam direction and integration into the structural system being controlled. This problem is best approached for each system configuration.

Acknowledgments

The authors wish to point out that the coarse system and its signal processing and the vibration sensor were conceived by Dr. C-C. Huang, and the multicolor CO_2 laser used in the fine system was conceived by Dr. N.E. Buholz. We wish to acknowledge the strong contributions of the following personnel of the Lockheed Missile and Space Co. in the development of these concepts: C.W. Gillard for fine system development; D.W. Ridder, T. Chang, W.M. Wells, and R.B. McIntosh for interface hardware and computer technology; L. Davis for analyses; and J.R. Hoder for breadboard assistance. The coarse sensor and vibration sensor were funded under LMSC independent development funds and the fine system by the Advanced Project Agency of the Department of Defense, under subcontract 9540-A-0002 to ITEK Corporation.

References

- ¹Huang, C-C., "Dual Bragg Cell Local Oscillator Generator for Laser Heterodyne Radar Systems," Paper TUC5, Conference on Laser and Electro-Optical Systems, San Diego, Calif., May 1976.
- ²Huang, C-C., "Structure Alignment Sensor," Lockheed Missiles & Space Company Tech. Rept. LMSC-D577453, Dec. 1977.
- ³Buholz, N.E., "Selected Time Color Operation of a CO_2 Laser," SPIE Technical Symposium East '80, Washington, D.C., April 7-11, 1980.
- ⁴Gillard, C.W., Buholz, N.E., and Ridder, D.W., "Absolute Distance Interferometry" SPIE Technical Symposium East '80, Washington, D.C., April 7-11, 1980.
- ⁵Huang, C-C. and Chang, T., "Vibration Sensor," Paper WCC9, Conference on Laser and Electro-Optical Systems, San Diego, Calif., Feb. 1980.